Supporting Information

Disclosing the Impact of Local Host Effects on TADF Dynamics

Björn Ewald,*[a] Theodor Kaiser,[a] Thomas Fleischmann[a] and Jens Pflaum*[a,b]

[a] *Experimental Physics 6, University of Würzburg, Am Hubland, 97074 Würzburg, Germany*

[b] *Center for Applied Energy Research e.V. (CAE), Magdalena-Schoch Straße 3, 97074 Würzburg, Germany*

Corresponding Authors

Björn Ewald - *Experimental Physics 6, University of Würzburg, Am Hubland, 97074 Würzburg, Germany*
https://orcid.org/0009-0000-7078-9252;
Email: bjoern.ewald@uni-wuerzburg.de

Jens Pflaum - *Experimental Physics 6, University of Würzburg, Am Hubland, 97074 Würzburg, Germany* - Center for Applied Energy Research e.V. (CAE), Magdalena-Schoch Straße 3, 97074 Würzburg, Germany
https://orcid.org/0000-0001-5326-8244
Email: jens.pflaum@uni-wuerzburg.de

SI 1: Single Molecule Spectra of TXO-TPA in PMMA

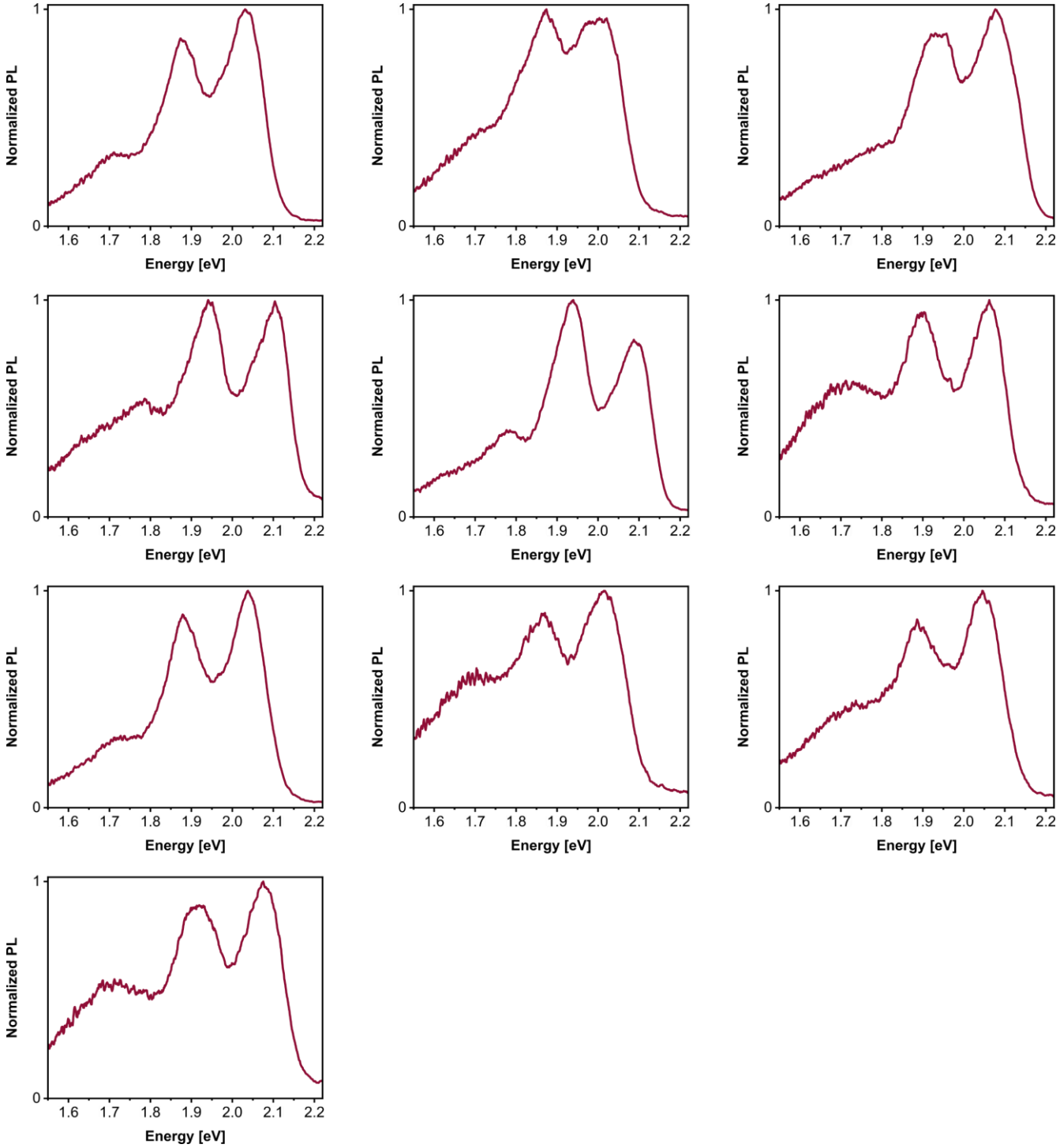

Figure S1. Normalized single molecule PL spectra of TXO-TPA dispersed in PMMA at ultralow concentrations of 10^{-8} wt%. Spectra of individual molecules are shown to illustrate the statistical distribution of spectral properties. The spectral data were post-processed by a moving average filter and a Jakobi transformation from the wavelength to the energy regime.

SI 2: Single Molecule Spectra of TXO-TPA in DPEPO

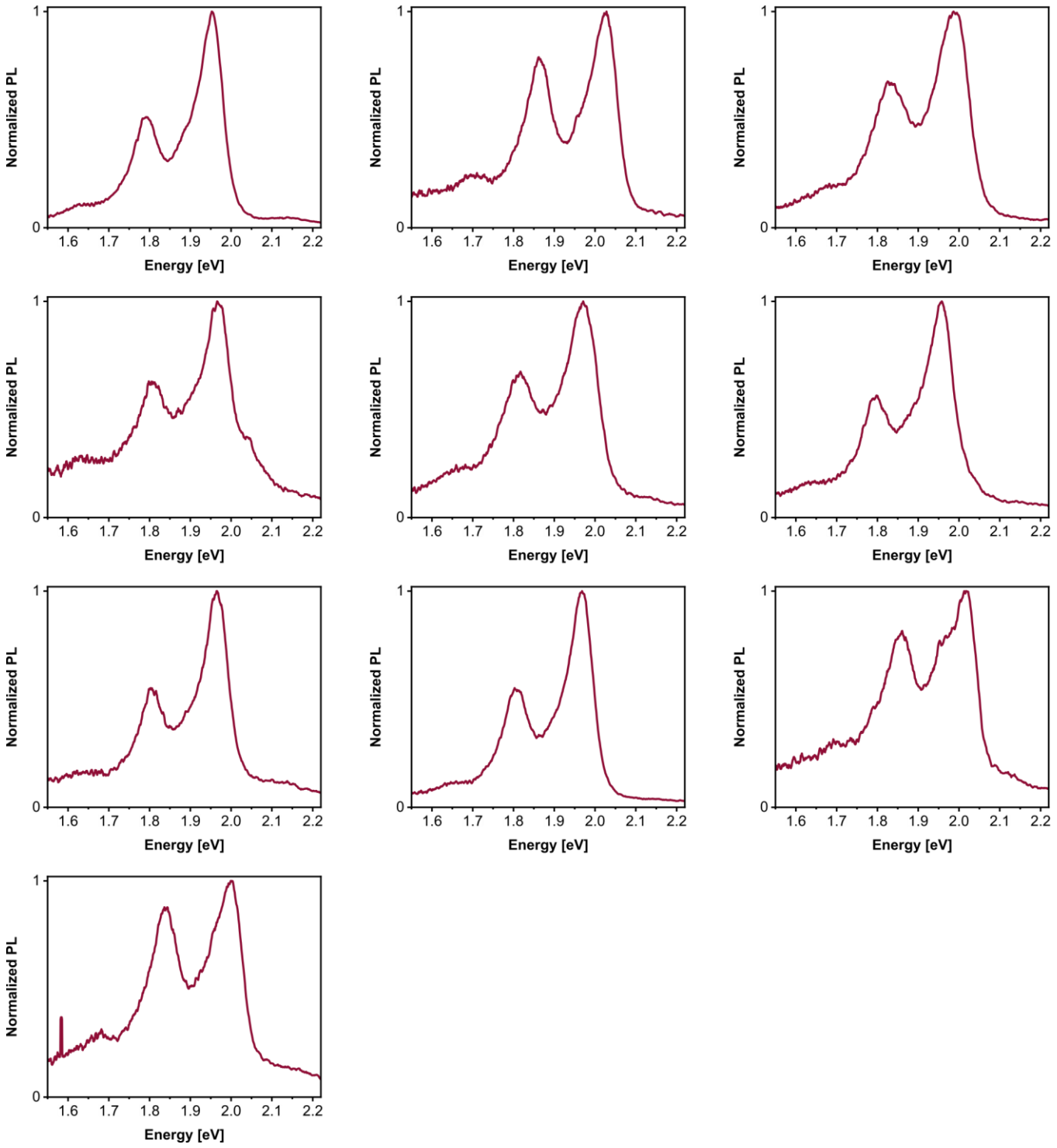

Figure S2. Normalized single molecule PL spectra of TXO-TPA dispersed in DPEPO at ultralow concentrations of 10^{-8} wt%. Spectra of individual molecules are shown to illustrate the statistical distribution of spectral properties. The spectral data were post-processed by a moving average filter and a Jakobi transformation from the wavelength to the energy regime.

SI 3: Single Molecule Spectra of TXO-TPA in UGH-3

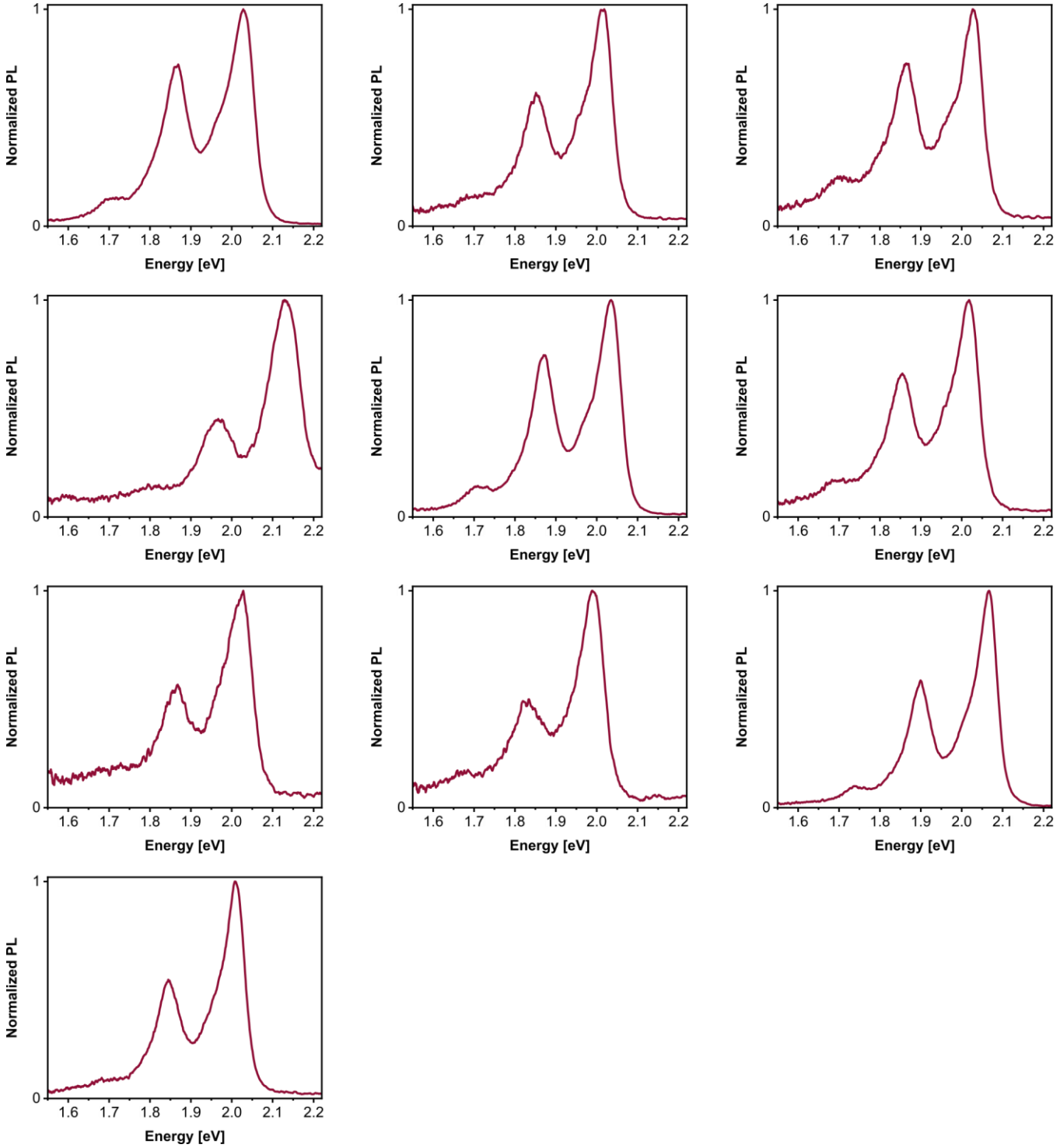

Figure S3. Normalized single molecule PL spectra of TXO-TPA dispersed in UGH-3 at ultralow concentrations of 10^{-8} wt%. Spectra of individual molecules are shown to illustrate the statistical distribution of spectral properties. The spectral data were post-processed by a moving average filter and a Jakobi transformation from the wavelength to the energy regime.

SI 4: Spectral Properties of Single TXO-TPA Molecules

The spectral properties of single TXO-TPA molecules in PMMA, DPEPO and UGH-3 are listed in Table S1. Given are the energetic positions of the 0-0, 0-1 and 0-2 transitions, as well as the Huang-Rhys parameter *S*. *S* was derived from the integral intensity ratio of the 0-0 and 0-1 transition:

$$S = \frac{I_{0-1}}{I_{0-0}} \quad \text{(SI1)}$$

Table S1. Spectral properties of single TXO-TPA molecules in the three host materials PMMA, DPEPO and UGH-3. The data were derived from a representative set of molecular entities (at least 10 single molecules). Given are the average energetic positions of the main vibronic transitions 0-0, 0-1 and 0-2, as well as the Huang-Rhys parameter *S* calculated from ratio of the integral intensities of the 0-0 and 0-1 transition.

Host Material	$E_{0\text{-}0}$ **(eV)**	$E_{0\text{-}1}$ **(eV)**	$E_{0\text{-}2}$ **(eV)**	***S***
PMMA	2.047 ± 0.037	1.906 ± 0.031	1.768 ± 0.029	1.01 ± 0.24
DPEPO	1.975 ± 0.024	1.826 ± 0.024	1.670 ± 0.027	0.66 ± 0.17
UGH-3	2.029 ± 0.040	1.871 ± 0.038	1.735 ± 0.039	0.58 ± 0.27

SI 5: Processing of Single Photon Correlation and Histogram Data

To account for uncorrelated background intensity I_B affecting the antibunching measurements, the corrected $g^{(2)}(\tau)$ correlation function was derived from the uncorrected $g_{uc}^{(2)}(\tau)$ function by the following equation:

$$g^{(2)}(\tau) = \frac{g_{uc}^{(2)}(\tau) - 1 + \left(\frac{I_M(t)}{I_M(t)+I_B}\right)^2}{\left(\frac{I_M(t)}{I_M(t)+I_B}\right)^2} \quad \text{(SI2)}$$

The background intensity I_B was measured on the neat host close to the single molecule spot and $I_M(t)$ corresponds to the time-dependent intensity at the single molecule position. The corrected antibunching data were fitted with the following mono-exponential function:

$$g^{(2)}(\tau) = 1 - C \cdot e^{-\frac{\tau}{\tau_a}} \quad \text{(SI3)}$$

Here τ_a is the effective antibunching lifetime and C is the magnitude of the antibunching at zero delay. As pointed out in the main part τ_a is not equal to the fluorescence lifetime in ensemble experiments. Only antibunching characteristics with $g^{(2)}(0) < 0.5$ were considered for the analysis. The two branches of the antibunching curves were fitted with a combined function.

The bunching data were utilized without post-processing. Bunching signatures were fitted with the following exponential decay function between 0.1 and 1000 µs:

$$g^{(2)}(\tau) = 1 + A \cdot e^{-\frac{\tau}{\tau_b}} \quad \text{(SI4)}$$

Here A is the bunching amplitude and τ_b the decay constant quantifying the characteristic bunching duration.

Histogram data were fitted with a (multi-)gaussian distribution function:

$$Prevalence = A \cdot e^{-\frac{(I-M)}{2\sigma^2}} \quad \text{(SI5)}$$

Here A is a scaled amplitude, I is the photon emission rate, M is the mean of the distribution, and σ is the standard deviation of the distribution.

SI 6: Photon Correlation and Histogram Data of TXO-TPA in PMMA

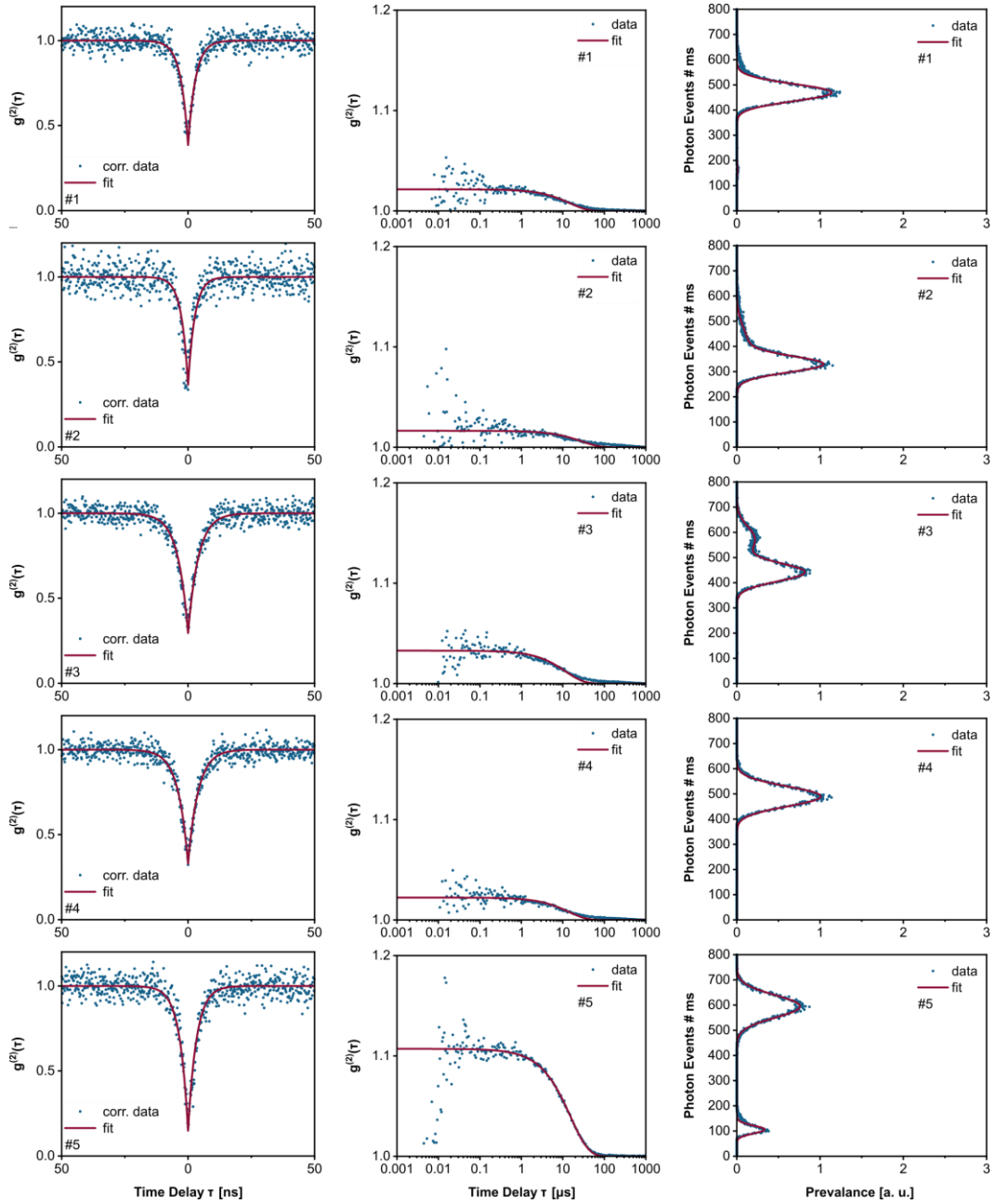

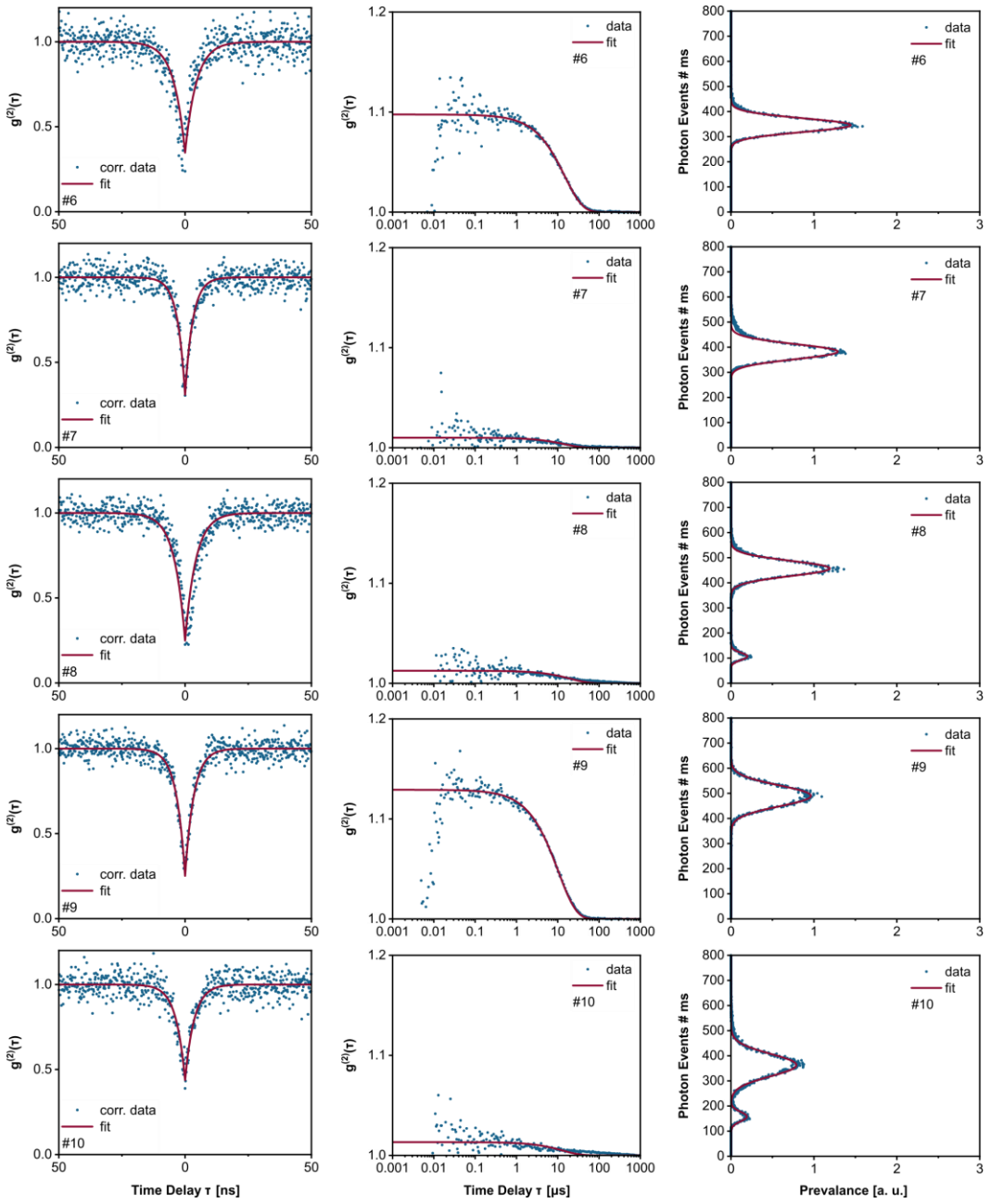

Figure S4. Photon correlation and histogram data of individual single TXO-TPA molecules in PMMA. Importantly antibunching data, bunching data and histograms of the photon emission rate were measured during the same lifetime cycle of the molecule. Left column: $g^{(2)}(\tau)$ correlation data in a time delay range between -50 and 50 ns. Shown are background corrected data (Equation SI2) and the corresponding exponential fits (Equation SI3). The antibunching characteristics with $g^{(2)}(0) < 0.5$ clearly confirm the single photon emission character of TXO-TPA. Middle column: $g^{(2)}(\tau)$ correlation data within a time delay of 1000 µs. Shown are the raw data without any post-processing and the corresponding exponential fits (Equation SI4) to the bunching decay. Bunching is present in correlation functions with $g^{(2)}(\tau)$ values larger than one on intermediate time scales. Right column: Histograms of the photon emission rate, derived from intensity time traces recorded during the photon correlation experiments with a time binning of 10 ms. The photon events per time are assigned to the prevalence of measuring the respective photon rate over different time bins. The raw data with the corresponding (multi-)gaussian fits (Equation SI5) are displayed. All measurements were carried out at 532 nm excitation wavelength and 300 µW cw excitation power with circularly polarized light.

SI 7: Photon Correlation and Histogram Data of TXO-TPA in DPEPO

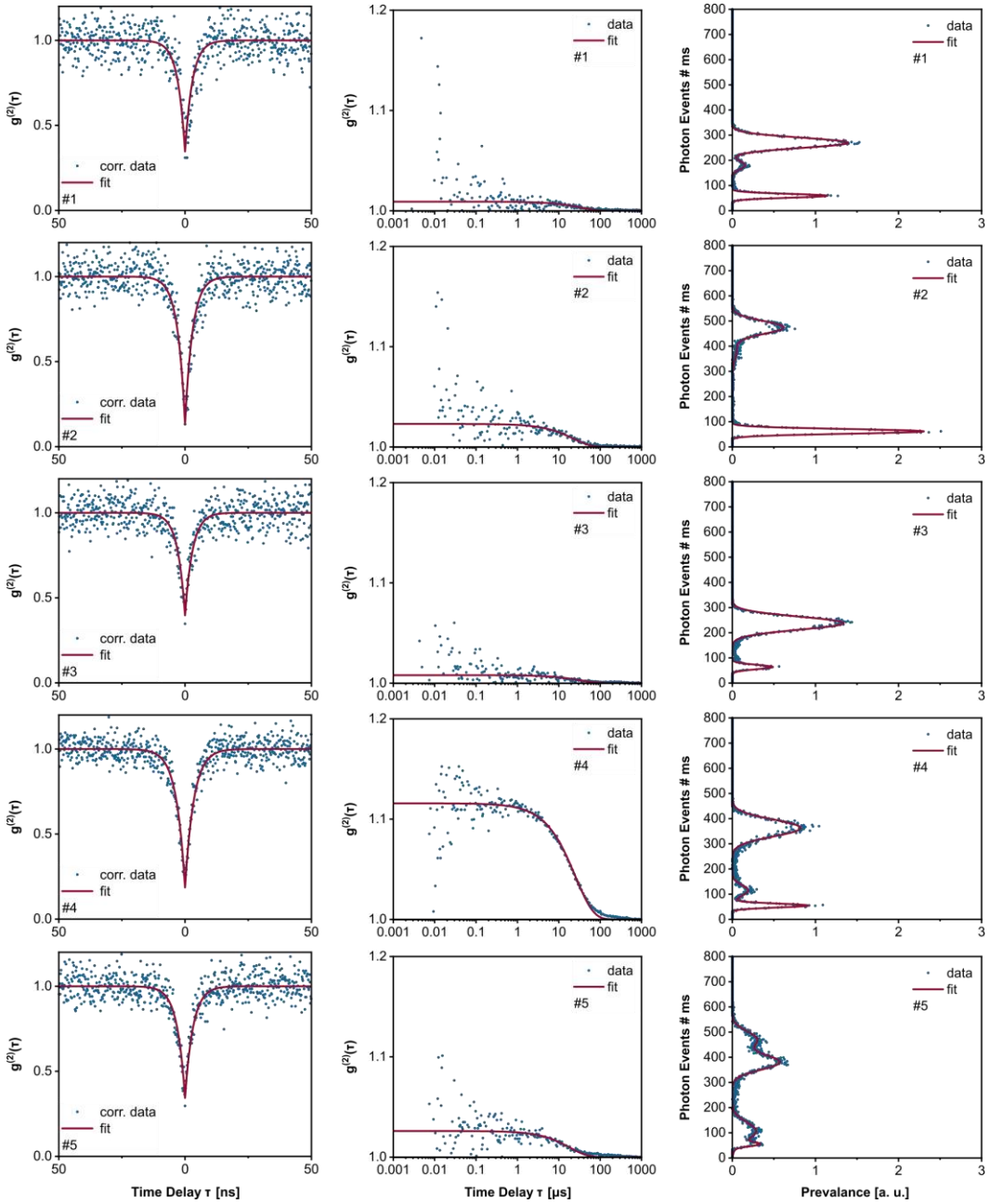

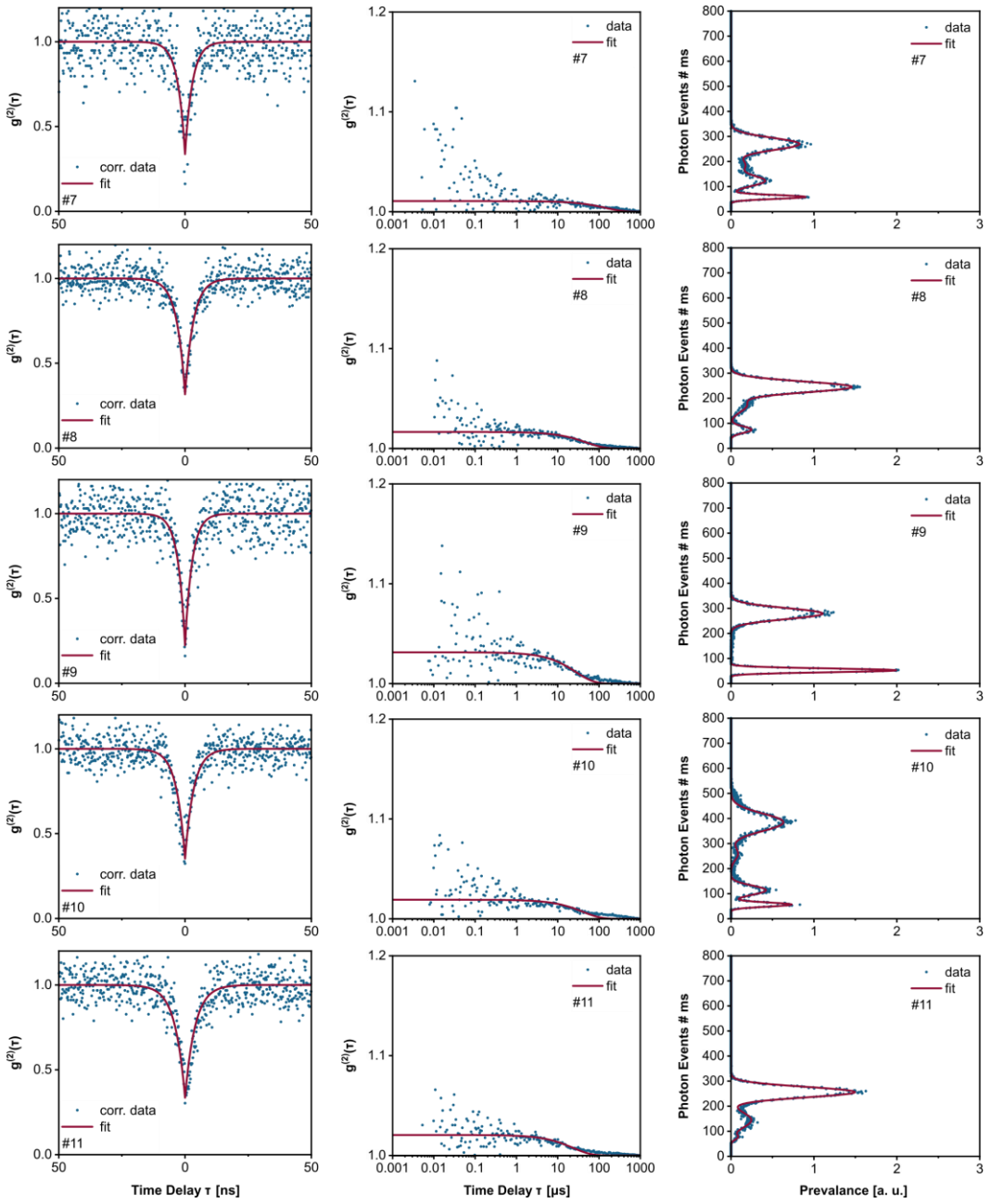

Figure S5. Photon correlation and histogram data of individual single TXO-TPA molecules in DPEPO. Importantly antibunching data, bunching data and histograms of the photon emission rate were measured during the same lifetime cycle of the molecule. Left column: $g^{(2)}(\tau)$ correlation data in a time delay range between -50 and 50 ns. Shown are background corrected data (Equation SI2) and the corresponding exponential fits (Equation SI3). The antibunching characteristics with $g^{(2)}(0) < 0.5$ clearly confirm the single photon emission character of TXO-TPA. Middle column: $g^{(2)}(\tau)$ correlation data within a time delay of 1000 µs. Shown are the raw data without any post-processing and the corresponding exponential fits (Equation SI4) to the bunching decay. Bunching is present in correlation functions with $g^{(2)}(\tau)$ values larger than one on intermediate time scales. Right column: Histograms of the photon emission rate, derived from intensity time traces recorded during the photon correlation experiments with a time binning of 10 ms. The photon events per time are assigned to the prevalence of measuring the respective photon rate over different time bins. The raw data with the corresponding (multi-)gaussian fits (Equation SI5) are displayed. All measurements were carried out at 532 nm excitation wavelength and 300 µW cw excitation power with circularly polarized light.

SI 8: Photon Correlation and Histogram Data of TXO-TPA in UGH-3

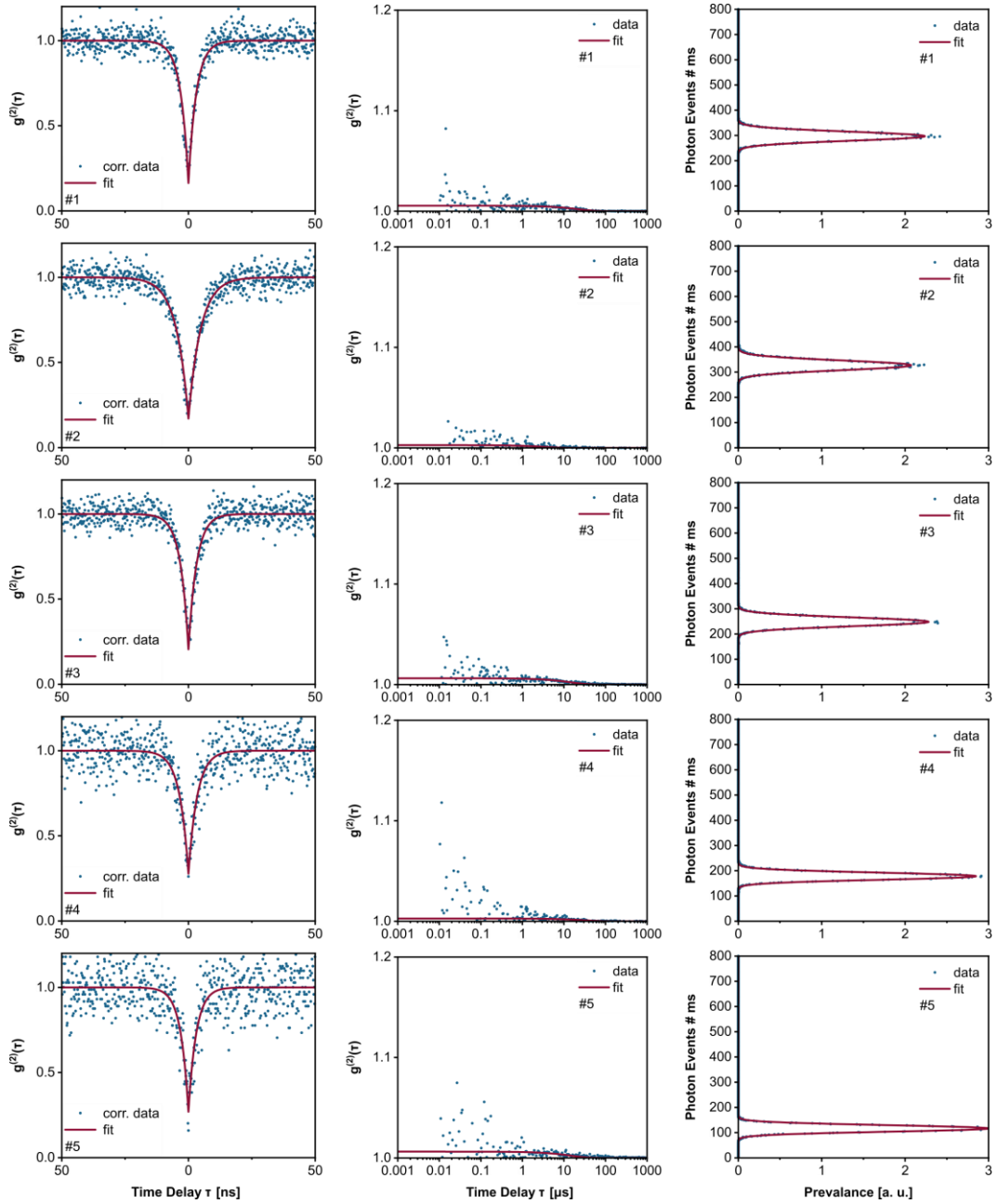

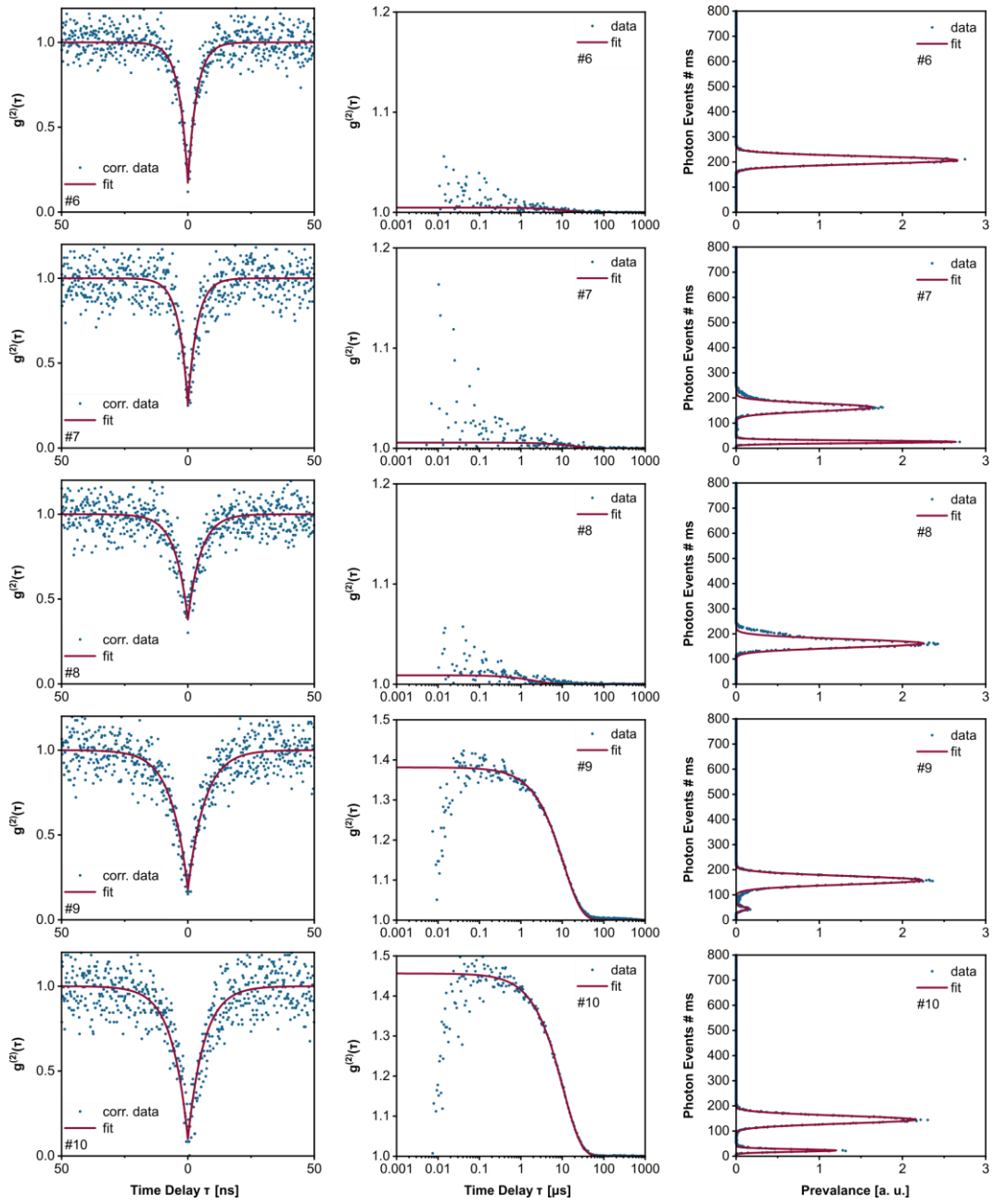

Figure S6. Photon correlation and histogram data of individual single TXO-TPA molecules in UGH-3. Importantly antibunching data, bunching data and histograms of the photon emission rate were measured during the same lifetime cycle of the molecule. Left column: $g^{(2)}(\tau)$ correlation data in a time delay range between -50 and 50 ns. Shown are background corrected data (Equation SI2) and the corresponding exponential fits (Equation SI3). The antibunching characteristics with $g^{(2)}(0) < 0.5$ clearly confirm the single photon emission character of TXO-TPA. Middle column: $g^{(2)}(\tau)$ correlation data within a time delay of 1000 µs. Shown are the raw data without any post-processing and the corresponding exponential fits (Equation SI4) to the bunching decay. Bunching is present in correlation functions with $g^{(2)}(\tau)$ values larger than one on intermediate time scales. Right column: Histograms of the photon emission rate, derived from intensity time traces recorded during the photon correlation experiments with a time binning of 10 ms. The photon events per time are assigned to the prevalence of measuring the respective photon rate over different time bins. The raw data with the corresponding (multi-)gaussian fits (Equation SI5) are displayed. All measurements were carried out at 532 nm excitation wavelength and 300 µW cw excitation power with circularly polarized light.

SI 9: Saturation of the Photon Emission Rate

We have measured the photon emission rate of single TXO-TPA molecules as function of the excitation power to identify a suitable excitation power density for photon correlation experiments and to determine the saturation regime of TXO-TPA within the three different hosts (PMMA, DPEPO and UGH-3). The saturation behavior of the emission rate (intensity I) as function of the excitation power P is described by the following equation with the saturation power P_S and the maximum emission rate I_∞:

$$I = I_\infty \cdot \left(\frac{P/P_S}{1+P/P_S}\right) \tag{SI6}$$

The corresponding power seria are shown in Figure S7 with the emission rate of the TXO-TPA molecules corrected by the host contributions, which are depicted in the bottom row.

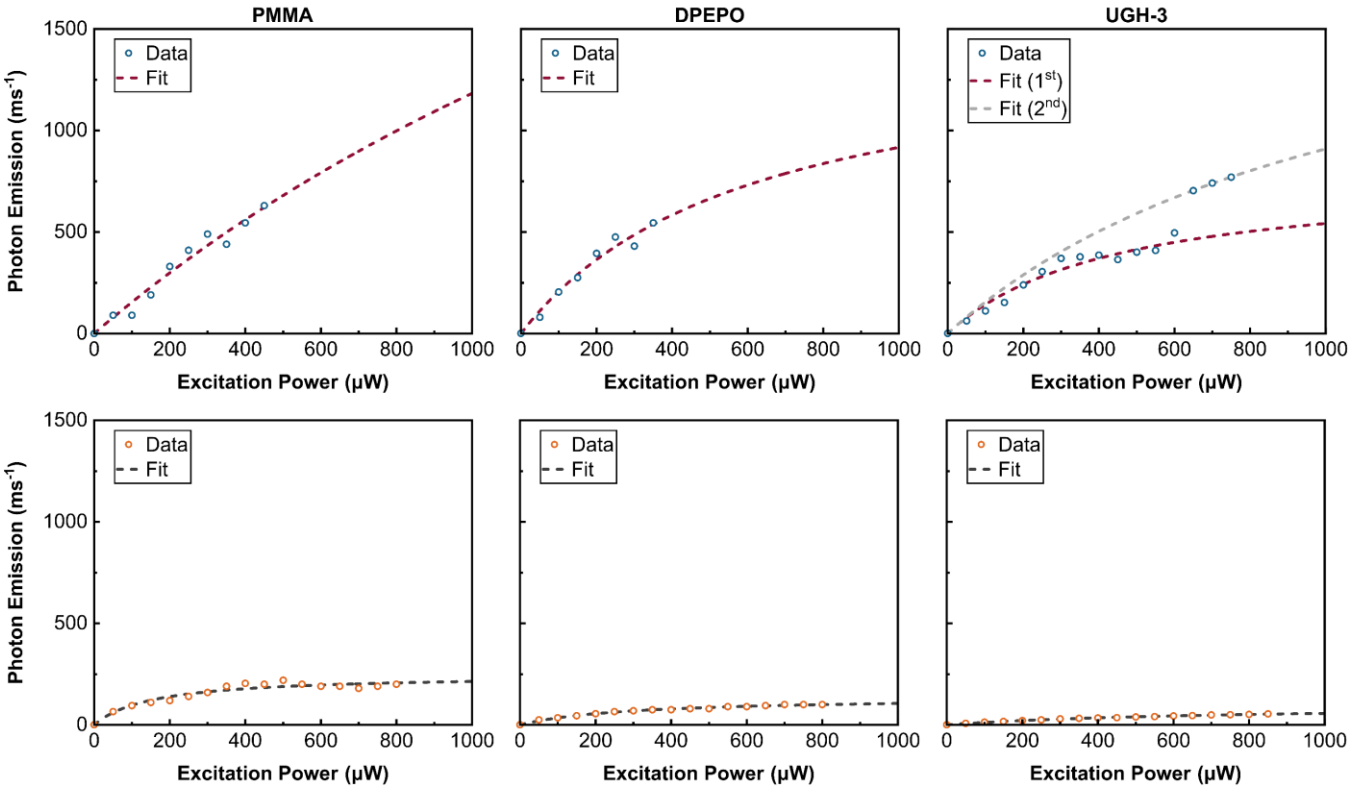

Figure S7. Photon emission rate of single TXO-TPA molecules in PMMA, DPEPO and UGH-3 (from left to right) as function of the excitation power. The top row corresponds to the power series of representative TXO-TPA molecules with the photon emission rate corrected by the host contribution. The parasitic background emission of the respective host material was measured on the neat host close to the single molecule spots (bottom row). Fits based on Equation SI6 are presented by dashed lines. In case of TXO-TPA in PMMA and DPEPO the fits are error-prone as the stability of single molecules in these hosts is limited to about 400 µW excitation power. In case of UGH-3 two different saturation regimes can be identified, which we attribute to softening of the host rigidity at excitation powers above 600 µW. This results in a behavior comparable to the flexible host materials. All measurements were carried out at 532 nm excitation wavelength with circularly polarized light. The excitation power was adjusted with a continuous grey filter wheel and measured with a power meter.

The parasitic background emission by the host is highest in PMMA, and lowest in UGH-3. In case of PMMA and DPEPO the fits are error-prone as the stability of single TXO-TPA molecules in these host materials is limited to an excitation power of about 400 µW. The fits should thus be considered more as a descriptive guide. In case of UGH-3 two different saturation regimes can be identified, which we attribute to softening of the host rigidity at excitation powers above 600 µW. Interestingly and consistently, the second saturation regime is then comparable to the non-rigid host materials. The uniform excitation power of 300 µW throughout the photon correlation measurements was chosen for the following reasons: 1.) A sufficient signal-to-background ratio must be ensured, which is the case at moderate and high excitation powers as the parasitic background contribution of the host is saturating. 2.) Excitation of TXO-TPA has to be close to saturation. 3.) Stability of the emitter entity has to be guaranteed during correlation experiments.

SI 10: Transient PL of TXO-TPA in the Emitter Ensemble

Ensemble thin film samples of TXO-TPA dispersed in PMMA, DPEPO and UGH-3 at an emitter concentration of 1 wt% were prepared (see experimental section). The confocal setup described in the experimental section was used for time-correlated single photon counting (TCSPC). A pulsed laser (λ_{ex} = 520 nm) and a hardware correlator (PicoHarp 300) synchronized by the electrical signal of the laser, together with an avalanche photodetector (Excelitas SPCM-AQRH-14, QE 65 % at 650 nm, dark counts < 100 counts·s^{-1}) were utilized to record histograms. The prompt and delayed fluorescence decay were measured with a laser pulse width of ~ 4 ns and ~ 36 ns, respectively. The instrument response function was measured with a cover glass at the sample position.

Lifetime density analysis was applied to analyze the prompt decay of TXO-TPA. A pseudo-continuous distribution of decay times is assumed:

$$I(t) = \sum_{\tau_i} a(\tau_i) \cdot e^{-\frac{t}{\tau_i}} * IRF(t) \qquad \text{(SI7)}$$

Here $I(t)$ is the photoluminescence signal, $a(\tau_i)$ are the amplitudes of the respective decay constants τ_i and $IRF(t)$ is the instrument response of the setup.

The prompt fluorescence decay together with the lifetime density distributions are shown in Figure S8. The mean fluorescence lifetimes are deduced from the maxima in the lifetime density distribution. The occurrence of three distinct maxima for the rigid UGH-3 host refers to a pronounced distribution of prompt lifetimes (0.5 ns, 2.8 ns and 21.1 ns) over the ensemble. These results are complementary to the antibunching measurements which revealed a distribution of the antibunching width in case of UGH-3. In PMMA and DPEPO the dominant lifetimes are 21.7 ns and 22.4 ns, respectively, and are comparable to the long component in UGH-3. An additional, less pronounced fast component of 1.4 ns can be identified in PMMA and DPEPO.

The transient PL measurements of the delayed component are displayed in Figure S9. An exponential decay was fitted to deduce the mean lifetime constant of the delayed fluorescence. The delayed lifetime is 13 µs in PMMA, 10 µs in DPEPO and 8 µs in UGH-3, which reveals a strong impact of the host material on the RISC/ISC dynamics. The ensemble data lack the direct information on local host-emitter interactions, which we gained from single molecule spectroscopy.

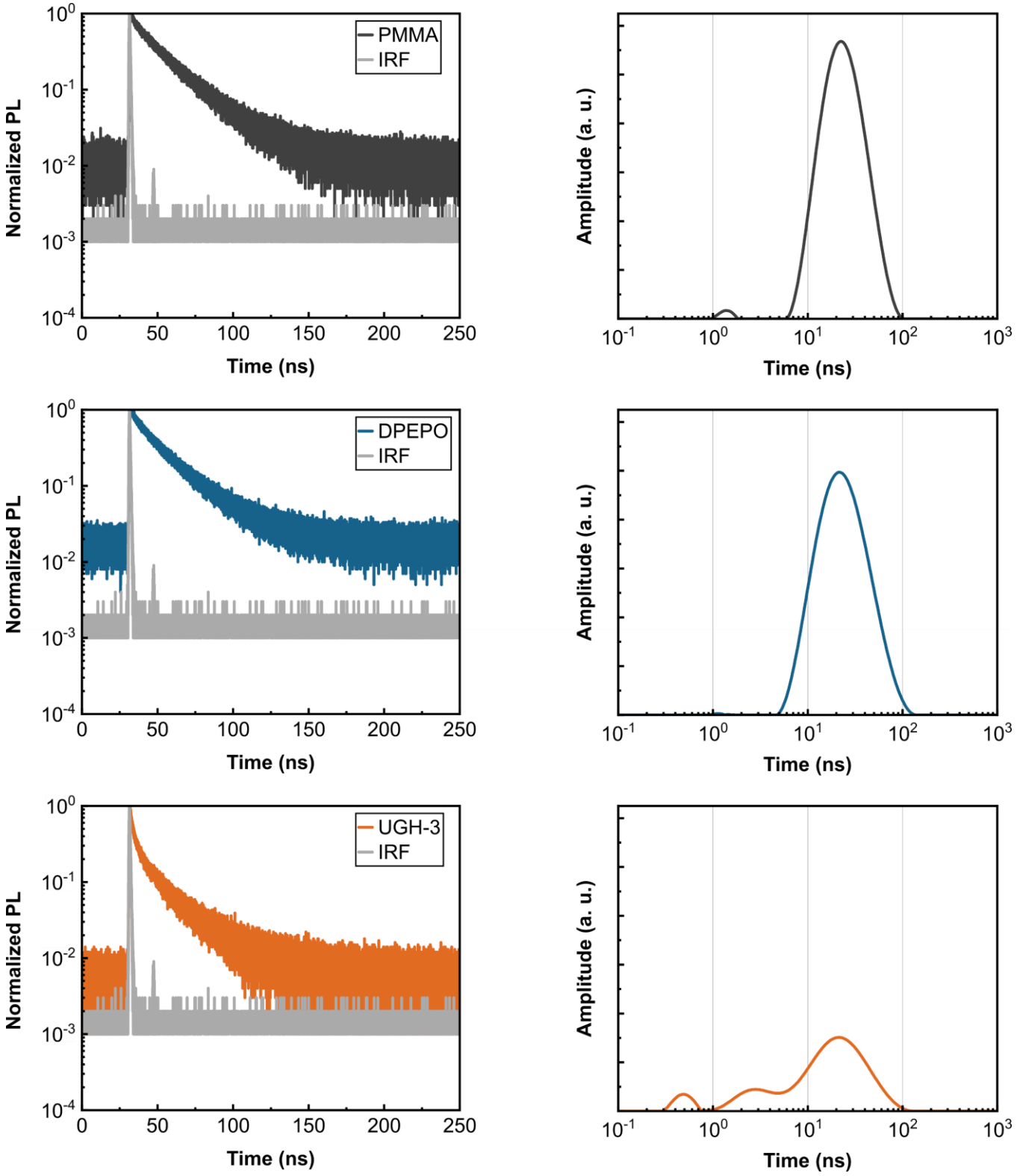

Figure S8. Transient PL measurements of the prompt fluorescence of TXO-TPA dispersed at 1 wt% concentration in PMMA, DPEPO and UGH-3 (from top to bottom). Left column: Normalized intensity histograms with the instrument response function (IRF) shown in grey. Right column: Corresponding lifetime density distributions (Equation SI7) of the prompt decay component.

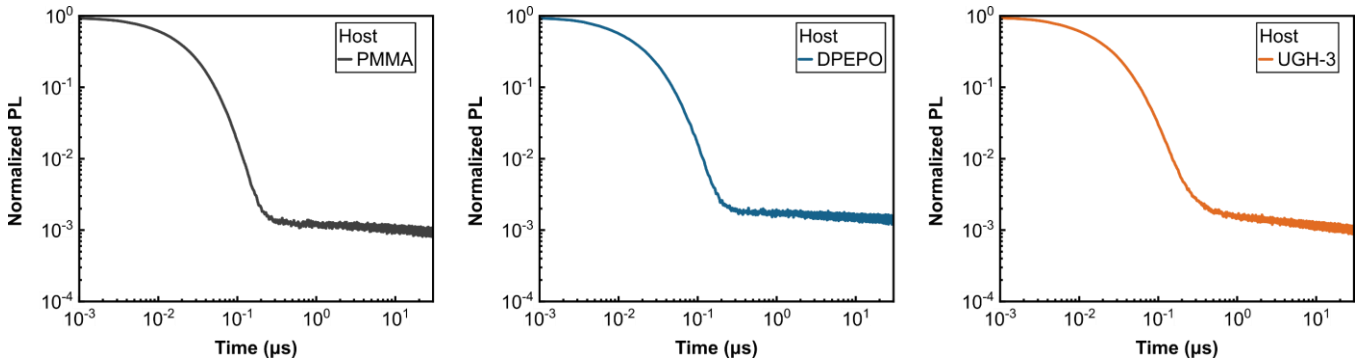

Figure S9. Transient PL measurements of the delayed fluorescence of TXO-TPA dispersed at 1 wt% concentration in PMMA, DPEPO and UGH-3 (from left to right). Shown are the normalized intensity histograms after applying a moving average filter to the raw data.

SI 11: Bunching Duration as a Function of the Dielectric Constant

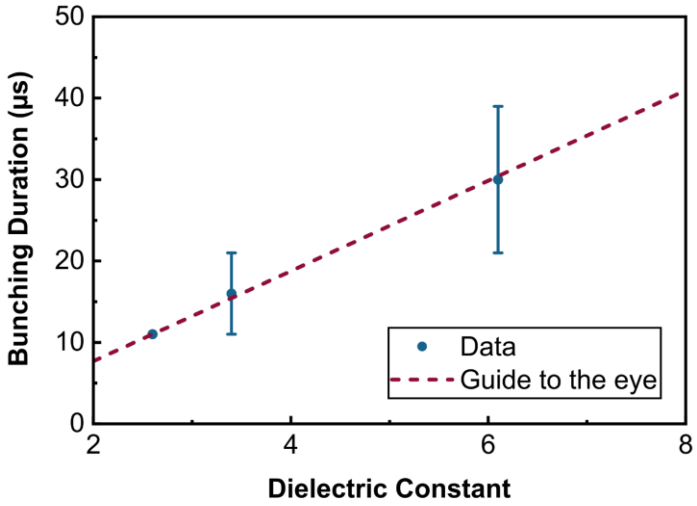

Figure S10. Bunching duration (τ_b) as a function of the dielectric constant (ε_r) of the host materials. The guide to the eye suggests a linear increase of τ_b with ε_r.